Available online at www.sciencedirect.com
ScienceDirect
Construction and Building Materials 23 (2009) 264–274
Construction and Building MATERIALS
www.elsevier.com/locate/conbuildmat

Experimental and numerical determination of the chloride penetration in cracked concrete

L. Marsavina [a,*], K. Audenaert [b], G. De Schutter [b], N. Faur [a], D. Marsavina [c]

[a] "Politehnica" University of Timisoara, Department Strength of Materials, Blvd. M. Viteazu, No. 1, Timisoara 300222, Romania
[b] Ghent University, Magnel Laboratory for Concrete Research, Department of Structural Engineering, Technologiepark-Zwijnaarde 904, B-9052 Ghent, Belgium
[c] RA Aquatim, Gh. Lazar Str., No. 11A, Timisoara 300081, Romania

Received 6 July 2007; received in revised form 16 December 2007; accepted 19 December 2007
Available online 21 February 2008

Abstract

One of the major causes of deterioration of reinforced concrete structures is chloride-induced corrosion of the reinforcing steel. This phenomenon is significantly influenced by the presence of cracks. This paper presents the experimental and numerical results on the influence of cracks on chloride penetration in concrete structures. The experimental results were obtained with the non-steady state migration test, described in NT BUILD 492, using an electrical field and artificial cracks. The numerical simulation results were obtained using a transient finite element analysis. A variable diffusion coefficient with total chloride concentration was considered in the simulation. A good agreement between experimental and the numerical chloride penetration results was obtained.

Keywords: Chloride penetration; Crack; Concrete; Experimental determination; Numerical simulation

1. Introduction

Chloride-induced steel corrosion is worldwide one of the major deterioration problems for reinforced concrete structures. The high alkaline environment of good quality concrete forms a passive film on the surface of the embedded steel which normally prevents the steel from further corroding. However, under chloride attack, the passive film is disrupted or destroyed, and the steel spontaneously corrodes [1]. The volume of rust products is about four to six times larger than that of iron. This volume increase induces internal tensile stresses in the cover concrete, and when these stresses exceed the tensile strength of the concrete, the cover concrete is damaged by cracking, delamination and spalling. In addition to loss of cover concrete, a reinforced concrete member may suffer structural damage due to loss of bond between steel and concrete and loss of rebar cross-sectional area.

Gowripalan et al. [2] studied the chloride diffusivity on concrete cracked in flexure. They concluded that crack width/cover ratio can be a suitable parameter to estimate the durability of a cracked reinforced concrete. Win et al. [3] determined the penetration profile of chloride in cracked reinforced concrete and found that the reinforced concrete specimens having cracks showed rapid penetration of Cl^- ion, which finally reached the steel. Penetration along the steel also occurred. All of these studies were based on experimental results.

Numerical studies were focused on developing a numerical algorithm in order to estimate the chloride penetration. Meijers [4] and Tang [5] used a mathematical model based on simulating free chloride penetration through the pore solution in concrete and calculating the distribution of the total chloride content in concrete. Truc et al. [6] present a numerical model, based on finite difference method and on the Nerst–Planck equation for the simulation of the

* Corresponding author. Tel.: +40 256 403577; fax: +40 256 403523.
E-mail address: msvina@mec.upt.ro (L. Marsavina).

0950-0618/$ - see front matter © 2008 Elsevier Ltd. All rights reserved.
doi:10.1016/j.conbuildmat.2007.12.015

transport of Cl^-, K^+, Na^+ and OH^- through saturated concrete during a migration test. Recently Martin-Perez et al. [7] proposed an algorithm based on modified Fick's second law for numerical modelling of transport of chlorides, moisture, oxygen and heat convection through concrete. Wang et al. [8] proposed a mathematical model for the simulation of an electrochemical chloride removal process in order to predict the ionic mass transport associated with chloride ingress into concrete or hydrated cement paste from a saline environment. Up to now not many simulations were performed in order to determine the chloride penetration in cracked concrete geometries.

At the Magnel Laboratory for Concrete Research from Ghent University several research programmes have been conducted concerning massive concrete armour units for breakwaters, especially dealing with thermal stresses due to heat of hydration leading to cracks. A new method for the study of the influence of cracks in concrete structures on carbonation and chloride penetration has been developed [9–11]. This method consists of the use of notches by means of the positioning and removal afterwards of thin copper sheets inside the specimen in the fresh concrete. After few hours, the copper sheets were removed and artificial cracks were created in the concrete. The notched specimens have been subjected to a non-steady state migration test. After the test, the specimens were axially split perpendicular to the notch and an $AgNO_3$ solution was sprayed in order to measure the chloride penetration depth.

In this paper, the chloride penetrations in three types of concrete with notches are described. A model is developed in order to numerically simulate the chloride penetration. A comparison between the numerical and experimental results will be presented.

2. Chloride penetration

The chloride ion transport in concrete can be modeled by a linear diffusion equation, Fick's second law, in the following form for one-dimension:

$$\frac{\partial C}{\partial t} = \frac{\partial}{\partial x} D \frac{\partial C}{\partial x}, \tag{1}$$

where C is the total chloride content, t time and D the diffusion coefficient. The following boundary conditions are considered:

- a single spatial dimension x, ranging from 0 to ∞ for the semi-infinite case,
- $C = C_0$ at $x = 0$ and $t > 0$ (boundary condition),
- $C = 0$ at $x > 0$ and $t = 0$ (initial condition).

Considering a constant diffusion coefficient an analytical solution of Eq. (1) has the form:

$$C = C_0 \left[1 - \operatorname{erf}\left(\frac{x}{2\sqrt{Dt}}\right)\right] \tag{2}$$

in which C_0 is a constant, erf() represents the error function.

The model used for chloride penetration based on Fick's second law and its error function solution is criticised because it is unable to take into account the concentration dependent diffusivity, and the depth dependent diffusivity, Tang [12]. Chatterji [13] proposed some modifications to Fick's law in order to be used for ion transport in cement based materials.

In the same time it should be mentioned that many analytical problems arise when Fick's second law is integrated for finite geometries with discontinuities like notches and cracks. This paper experimentally and numerically investigates the influence of cracks on chloride penetration.

3. Experimental programme

3.1. Concrete composition

Three types of concrete were investigated: Type 1 is a 5 year old completely carbonated concrete with blast furnace slag cement (CEM III/B 32.5 HSR LA). Type 2 and 3 are non-carbonated concrete mixes, having the same W/C ratio and based on ordinary Portland cement (CEM I 52.5 N). Type 2 and Type 3 have a cement content of 300 kg/m^3 and 400 kg/m^3 respectively. For Type 2 and 3, eight concrete batches have been produced, one for each notch configuration (see Section 3.2). For these mixes, the slump and density were measured in fresh condition. The compressive strength (on cubes with side length 150 mm) and density of the hardened concrete were measured at the age of 28 days. For these properties, the mean values are given in Table 1. For each mix, three concrete cubes side 150 mm were cast for the determination of the compressive strength together with 20 specimens for the determination of the chloride penetration. The concrete specimens were stored in a climate room at 20 ± 2 °C and more than 90% R.H. until the testing age.

Table 1
Concrete composition and properties

	Type 1	Type 2	Type 3
Composition			
CEM III/B 32.5 HSR LA (kg/m^3)	300		
CEM I 52.5 N (kg/m^3)		300	400
Sand 0/4 (kg/m^3)	670	670	585
Gravel 4/14 (kg/m^3)	1280		
Gravel 2/8 (kg/m^3)		490	430
Gravel 8/16 (kg/m^3)		790	690
Water (kg/m^3)	150	150	200
Fresh properties			
Slump (mm)		19	224
Density (kg/m^3)		2415	2375
Hardened properties			
$f_{ccub,28d}$ (N/mm^2)	30.4	57.4	49.6
Density (kg/m^3)		2390	2365

3.2. Crack formation

3.2.1. Literature review

In the literature, various research programmes concerning the influence of cracks on the chloride penetration are described, focussing on very different aspects. In these researches, different methods were used to create cracks. Two large groups are distinguished: natural cracks and artificial cracks. The main advantage of natural cracks is that they reproduce reality. However, some disadvantages should be noticed: firstly, it is very complicated to model the experimental results unless very far-reaching simplifications are introduced. Secondly, different methods are used to create real cracks. They can be roughly divided into four different groups:

- the Brazilian splitting test, which consists of creating tensile cracks in a concrete core or disk subjected to diametral compression, as described in [14–17]. For this type of test, linear variable displacement transducers (LVDT's) are used, together with a feedback displacement controlled test machine;
- the wedge splitting tests were used in many researches in the field of fracture mechanics because of the rather easy analytical description of the crack formation [18]. This type of test is also used in concrete research [19–22];
- three- or four-point bending tests on concrete prisms or beams as investigated by [3,23–26]. For the study of long term processes, such as the penetration of chlorides into cracked concrete, sometimes groups of 2 or 3 prisms loaded in three- or four-point bending are used: [2,24,27];
- ring-shaped test set-ups with an expansive core [28].

Of course, many variations are possible on each of the four types of tests and other test methods exist [29,30]. Therefore, it is not always easy to compare experimental results.

Also the artificial cracks have a major disadvantage: they do not exactly reflect reality, e.g., the surface of the notches contains more cement than the surface of a real crack, they are not tortuous,... Nevertheless, they are far easier to model, leading to interesting conclusions that are also applicable on real cracks [9].

In this paper, the first test results of a research programme dedicated to the influence of cracks on the penetration of chlorides and the resulting service life are described. In this stage, artificial cracks are considered in order to simplify the modelling of the test results.

3.2.2. Notch configuration

As shown in Fig. 1, concrete specimens were made with artificial cracks by means of the positioning and removal after approximately 4 h of thin copper sheets inside the specimen. These copper sheets had a thickness of 0.2 mm, 0.3 mm or 0.5 mm. The copper plates were placed at a depth in the concrete of 5 mm, 10 mm, 15 mm or 20 mm. The combinations of crack width and crack depth studied

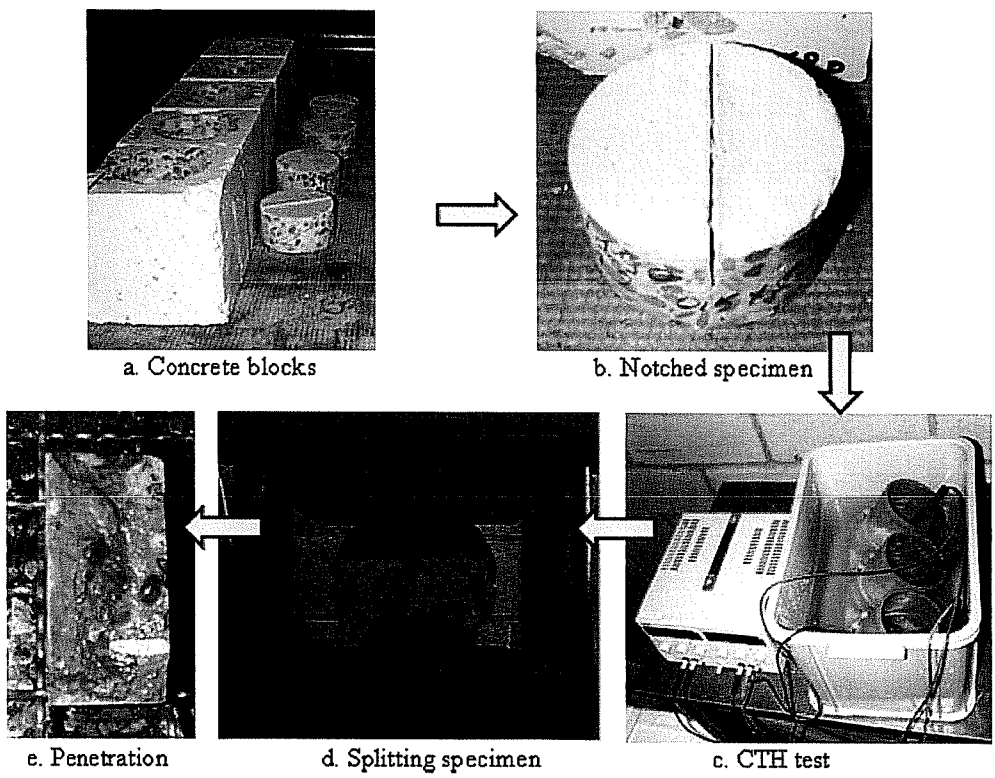

Fig. 1. Experimental procedure.

Table 2
Combinations of crack width and crack depth

Crack depth (mm)	Crack width (mm)			
	0	0.2	0.3	0.5
0	T1, T2 & T3			
5		T1, T2 & T3	T1, T2 & T3	
10		T2 & T3	T1, T2 & T3	
15		T2 & T3	T2 & T3	
20		T2 & T3	T2 & T3	T1

in this research are given in Table 2. Zero crack width and depth means that no crack is present. After hardening of the concrete specimens, cores were drilled from the concrete surface with a diameter of 100 mm and a thickness of 50 mm (Fig. 1b).

3.3. Chloride penetration

The ingress of chloride ions into concrete occurs in different ways: capillary suction, diffusion, migration,... or combinations of these transport mechanisms. In this research, the non-steady state migration test is used for the chloride penetration, leading to results within a few hours. Chloride diffusion tests are also initiated, but it will take much longer time period to obtain experimental results. In a next step, both methods will be compared.

As described in Section 3.1, cores with a diameter of 100 mm and a height of 50 mm were drilled from each cube. Afterwards the concrete cores were placed back in the fog room until the testing date. On these cores a non-steady state migration test was performed following the method of Tang et al. [31] as described in NT BUILD 492 [32] and shown in Figs. 1c and 2. The correspondence of this method with the natural ingress of chlorides by diffusion was validated in previous research carried out at the Magnel Laboratory for Concrete Research, Ghent University [33,34].

Before testing the specimens were vacuum saturated with a saturated $Ca(OH)_2$ solution. Afterwards an external electrical potential (25 V for concrete Type 2 and 3, 35 V or 40 V for Type 1) was applied across the specimen for a limited duration, forcing the chloride ions from the 10% NaCl solution (catholyte) to migrate into the specimens. For the un-notched specimens, the test duration was 24 h, as prescribed by NT BUILD 492 [32]. For the notched specimens the test duration was shortened in order to prevent complete penetration. For the concrete Type 1, only few specimens were available. For this reason, test durations of 4 or 6 h were chosen and specimens with different notch configurations were tested simultaneously. For the concrete Type 2 and 3, 20 specimens were available for each notch configuration for each concrete type. For this reason, the test duration was varied from 2 to 4, 6, 8 and 10 h. Three specimens were tested for each of test duration. In this way, the evolution of the penetration front can be visualized.

After the test, the specimens were axially split, perpendicular to the notch (Fig. 1d). On each of the freshly split sections, a 0.1 M $AgNO_3$ solution was sprayed and the chloride penetration depth is measured at 15 points, visually checking the presence of white silver chloride precipitation (Fig. 1e). This colorimetric method is described in [35]. For each concrete core, two penetration profiles were obtained. In this way, 6 penetration profiles are obtained for each composition and notch configuration. The mean penetration profile for crack width 0.3 mm and crack depth 20 mm for Type 3 is given in Fig. 3 (the test results are already converted to the reference age of 28 days, as explained in Section 3.4). On the horizontal axis, the

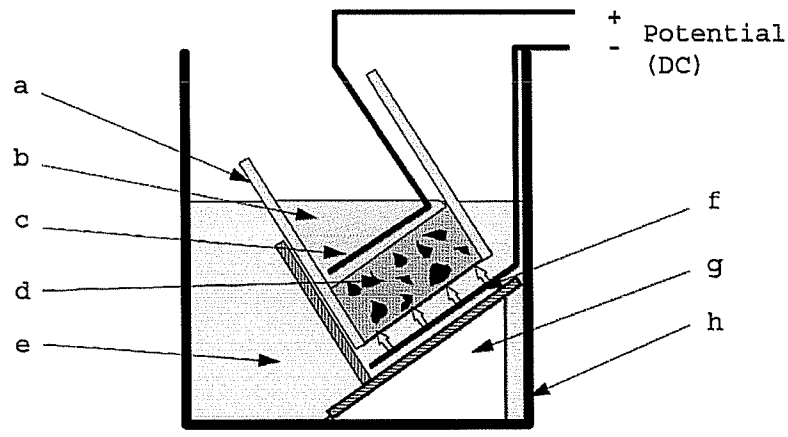

Fig. 2. Test method developed by Tang [12].

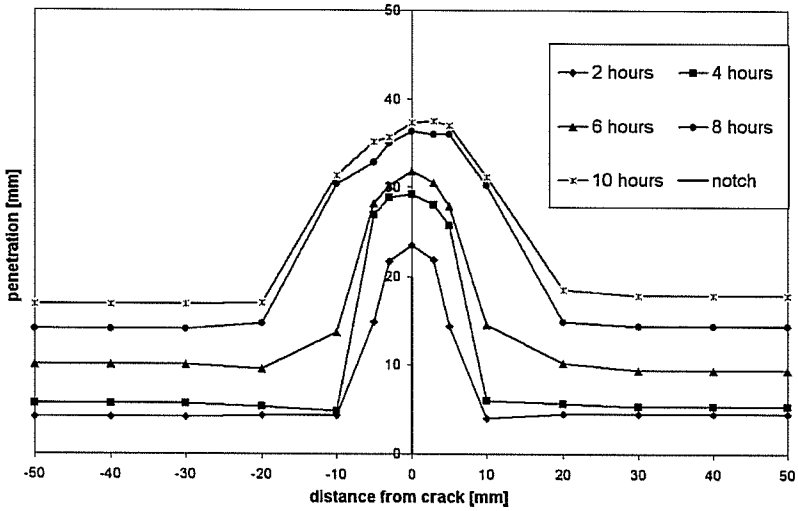

Fig. 3. Chloride penetration depth for crack width 0.3 mm and crack depth 20 mm for Type 3.

distance to the crack (or notch) is given. Distance 0 indicates the crack location.

From the penetration profile, the non-steady state D_{nssm} chloride migration coefficient can be calculated, as described in NT BUILD 492 [32], with:

$$D_{nssm} = \frac{RT}{zFE}\frac{x - \alpha\sqrt{x}}{t} \tag{3}$$

$$\text{with : } E = \frac{U-2}{L} \text{ and } \alpha = 2\sqrt{\frac{RT}{zFE}}\text{erf}^{-1}\left(1 - \frac{2C_d}{C_0}\right)$$

D_{nssm} non-steady state migration coefficient, m^2/s
z absolute value of ion valence, for chloride: $z = 1$
F Faraday constant $= 9.648 \times 10^4$ J/(V mol)
U absolute value of the applied voltage, V
R gas constant, $R = 8.314$ J/(K mol)
T average value of the initial and final temperatures in the anolyte solution, K
L thickness of the specimen, m
x average value of the penetration depths, m
t test duration, s
C_d chloride concentration at which the colour changes, $C_d = 0.07$ N for Portland cement concrete
C_o chloride concentration in the catholyte solution, $C_o = 2$ N

The value of the non-steady state migration coefficient was used for the numerical simulation in the second part of the paper.

3.4. Influence of testing age

As written in the literature [36–38], the diffusion and the migration coefficient of concrete are decreasing with concrete age. This has a significant influence on the measured penetration depth. As the CTH tests were not carried out on a constant concrete age, a correction is needed in order to compare the penetration depths. A reference concrete age of 28 days was chosen. The equation mostly used for the influence of age on the migration coefficient in the literature [31,38–40] is

$$D(t) = D_1 t^{-m} \tag{4}$$

with D_1 the value at an age of 1 year (m^2/s) and m a constant (–). Based on test results from earlier testing programmes on pure Portland cement concrete [33,41], a value of 0.27 for m was used. This value agrees very well with values from the literature [36,37].

The relation describing the chloride concentration in function of the distance from the concrete surface is given in Eq. (2). Combining Eqs. (2) and (4), the following equation is obtained, giving the penetration depth at a concrete reference age of 28 days in function of the measured penetration depth at a concrete age t:

$$x_{28} = x_t\sqrt{\frac{D_{28}}{D_t}} = x_t\sqrt{\left(\frac{28}{t}\right)^{-0.27}} = x_t\left(\frac{28}{t}\right)^{-0.135} \tag{5}$$

With this formula, the chloride penetration depths at the reference age of 28 days are calculated from the measured chloride penetration depths. This method is not applied for the concrete Type 1 because is this case no value for m is available. Type 1 is not a pure Portland cement based concrete and moreover it is completely carbonated concrete.

3.5. Test results

In order to analyse the test results from the chloride penetration profiles, the information of each profile was reduced to 3 figures: the maximum and mean penetration depth and the penetration depth in the end zones. The maximum penetration depth of the crack zone is calculated as the mean value of the penetration depths at the notch

and at 3 mm distance from the notch. These values are given in Table 3. In Table 4, the mean of the whole penetration front is determined. The mean value in the end zones (from −50 mm to −30 mm and from 30 mm to 50 mm), which are supposed not to be influenced by the notch, is given in Table 5.

The values of Type 1 are not corrected for the concrete age and are consisting of a very limited number of chloride profiles. Also the voltage applied is differing from Type 2 and 3 (see Section 3.1). For this reason, no direct comparison between Type 1 on the one hand and Type 2 and 3 on the other hand is possible.

The chloride profiles for concrete Type 2 with a notch width of 0.2 mm will be presented in the next section together with numerical results. The depth of the notch is indicated in the figures. The penetration depths are drawn for half a specimen. In this way, each point is representing the mean value of 12 measurements.

3.6. Discussion of test results

From the chloride penetration profiles, four influencing factors will be studied: test duration, crack width, crack depth and cement content.

3.6.1. Influence of test duration

The chloride penetration profile is strongly influenced by the test duration (see Fig. 3). Overall, the longer the test duration, the higher the penetration depth was obtained, as could be expected. However, most interesting is the evolution of the chloride penetration front. For the larger test durations, the chloride penetration front has flattened. This result is also obtained by the numerical modelling (see Section 4.3).

Table 3
Maximum penetration depth (mm)

	Crack width (mm)	Crack depth (mm)	Duration of test (h)				
			2	4	6	8	10
Type 1[a]	0.5	20		48.2	43.5		
	0.3	5		46.0	35.5		
	0.3	10		46.8			
	0.2	5			39.5		
Type 2	0.3	5	10.4	13.4	17.2	16.6	16.7
	0.3	10	10.0	12.2[b]		20.8	30.6
	0.3	15	12.4	25.0	25.1	27.6	35.3
	0.3	20	26.0	29.8	35.1	31.8	33.5
	0.2	5	10.4	15.2	18.6	19.3	29.2
	0.2	10	14.0	24.4	29.8	27.3	26.7
	0.2	15	19.2	22.1	22.5	30.1	34.2
	0.2	20	26.4	32.7	36.3	31.1	36.4
Type 3	0.3	5	5.4	8.5	12.3	16.3	17.7
	0.3	10	6.0	10.8	14.5	22.1	22.9
	0.3	15	17.3	21.2	25.5	26.8	33.2
	0.3	20	24.1	30.9	33.3	38.6	39.7
	0.2	5	7.1	9.8	12.1	12.4	15.8
	0.2	10	8.2	14.4	16.7	15.9	22.6
	0.2	15	14.5	20.2	24.7	21.8	26.3
	0.2	20	9.5	22.7	25.7	28.4	33.4

[a] 35 V was applied for the test of 4 h and 40 V for the test of 6 h.
[b] Test duration 5 h.

Table 4
Mean penetration depth (mm)

	Crack width (mm)	Crack depth (mm)	Duration of test (h)				
			2	4	6	8	10
Type 1[a]	0.5	20		43.8	37.0		
	0.3	5		45.3	35.4		
	0.3	10		43.8			
	0.2	5			36.1		
Type 2	0.3	5	6.2	9.6	13.9	13.6	14.8
	0.3	10	5.3	8.7[b]		15.6	23.8
	0.3	15	6.7	10.7	14.8	17.9	25.6
	0.3	20	11.5	13.1	19.4	18.0	19.9
	0.2	5	7.3	10.4	13.4	16.7	25.8
	0.2	10	8.9	16.2	20.0	18.6	21.6
	0.2	15	8.9	12.3	13.4	19.1	24.7
	0.2	20	11.2	18.2	18.9	19.0	21.8
Type 3	0.3	5	4.9	7.7	11.7	15.0	17.1
	0.3	10	4.8	8.5	10.1	15.8	18.5
	0.3	15	7.1	11.8	16.7	18.3	21.7
	0.3	20	10.0	13.9	18.3	25.2	27.7
	0.2	5	4.6	8.1	11.9	12.3	15.8
	0.2	10	5.0	9.1	11.6	13.1	19.2
	0.2	15	6.8	11.9	15.1	14.9	19.4
	0.2	20	5.3	11.4	13.9	18.0	22.9

[a] 35 V was applied for the test of 4 h and 40 V for the test of 6 h.
[b] Test duration 5 h.

Table 5
Mean penetration depth in end zones (mm)

	Crack width (mm)	Crack depth (mm)	Duration of test (h)				
			2	4	6	8	10
Type 1[a]	0.5	20		40.6	33.1		
	0.3	5		45.7	36.1		
	0.3	10		42.1			
	0.2	5			35.1		
Type 2	0.3	5	3.2	6.3	11.2	12.8	13.6
	0.3	10	2.8	5.9[b]		11.7	15.0
	0.3	15	4.3	5.5	8.5	11.6	16.1
	0.3	20	4.9	4.4	10.5	10.4	13.4
	0.2	5	5.5	9.0	10.8	18.2	23.3
	0.2	10	5.8	11.7	15.0	16.3	19.2
	0.2	15	5.5	7.9	10.7	14.0	19.5
	0.2	20	4.7	11.0	11.9	13.3	15.1
Type 3	0.3	5	4.6	7.2	11.4	13.9	16.9
	0.3	10	4.5	7.9	8.3	13.1	16.4
	0.3	15	3.4	7.8	12.0	13.9	15.5
	0.3	20	4.7	5.9	10.4	15.3	18.7
	0.2	5	3.6	7.5	11.8	12.2	15.8
	0.2	10	4.1	6.9	9.8	12.0	17.4
	0.2	15	4.4	8.0	11.0	11.7	16.0
	0.2	20	4.3	7.3	9.0	13.3	17.0

[a] 35 V was applied for the test of 4 h and 40 V for the test of 6 h.
[b] Test duration 5 h.

3.6.2. Influence of crack width

The influence of the crack width is less pronounced. For Type 3 and in earlier research [4,5], studying the chloride penetration by immersion in mortar prisms with notches, smaller crack widths lead to smaller penetration depths. By studying Tables 4–6, this is not clear for Type 2.

3.6.3. Influence of crack depth

Both for Type 2 and Type 3 and for both crack widths, a higher chloride penetration depth is noted for a higher crack depth. This is more pronounced for longer test durations. It is also interesting to study the additional chloride penetration depth. This depth is calculated as the distance between the crack tip and the chloride penetration front. This value is decreasing for increasing crack depth. For example, for a test duration of 10 h, concrete Type 2 and a crack width of 0.2 mm, the additional chloride penetration depth is decreasing from 10.8 (15.8–5 mm) for a crack depth of 5–2.9 mm (22.9–20 mm) for a crack depth of 20 mm. This shows that, even though the tortuosity of the cracks is not studied by using notches, the chloride ions do need a certain time to bridge the crack depth.

3.6.4. Influence of amount of cement

By increasing the amount of cement from 300 kg/m^3 for Type 2 to 400 kg/m^3 for Type 3 at a constant W/C ratio, the maximum and mean penetration depth are decreasing. This could be explained by the higher amount of chlorides that is bound to the cement matrix.

4. Numerical simulation

4.1. Simulation method

The finite element method was used to numerically solve the diffusion Eq. (1). For the numerical simulation the COSMOS/FFE Thermal software was used to investigate the chloride penetration in concrete specimens. The COSMOS/FFE Thermal is a fast, robust, and accurate finite element program for the analysis of linear and nonlinear, steady state and transient heat conduction problems with convective and radiative type boundary conditions in one-, two-, and three-dimensional geometries, [42]. The governing equation for the COSMOS/Thermal FFE module is

$$\rho C_S \frac{\partial T}{\partial t} = \frac{\partial}{\partial x} K_x \frac{\partial T}{\partial x} + \frac{\partial}{\partial y} k_y \frac{\partial T}{\partial y} + \frac{\partial}{\partial z} k_z \frac{\partial T}{\partial z} + Q \quad (6)$$

where T is the temperature, t represents the time, ρ is the density, C_S is the specific heat, k_x, k_y, k_z are the thermal conductivities in global x, y and z-directions, and Q represents the heat generation rate. Eq. (6) is similarly with Eq. (1) if we consider $\rho = C_S = 1$ and $Q = 0$. For simulation of chloride penetration the temperature T is replaced by the total concentration C, and the thermal conductivity k_x by diffusion coefficient D. The COSMOS package allows modelling of temperature dependent material properties. In present simulation a concentration dependent diffusion coefficient was used.

A transient analysis was used. Transient analysis implies that total concentration at any given point in the medium varies with time. A non-linear analysis was performed, due to the concentration dependency of the diffusion coefficient. The Newton–Raphson method was used for the iterative solution of the resulting set of non-linear equations, [42].

4.2. Simulation parameters

Four notched geometries were considered for the numerical simulation according to Table 6. Based on symmetry and in order to reduce the size of the model a quarter of cylinder was modeled. Solid 3D-8 node linear elements were used for meshing the model. A convergence study was carried out in order to determine the proper mesh density, and the element size of 1 mm was considered acceptable. The model geometry with a notch of 5 mm depth and 0.2 mm width is shown in Fig. 4.

The boundary conditions were applied on the model edges as following: the insulation boundary condition (0 flux) for the lateral edges and the applied total chloride

Table 6
Geometries and mesh parameters for numerical simulations

Geometries	Crack dimensions		Mesh parameters	
	Depth (mm)	Width (mm)	Number of elements	Number of nodes
I	5	0.2	82,250	87,567
II	10	0.2	82,000	87,312
III	15	0.2	81,750	87,057
IV	20	0.2	81,500	86,802

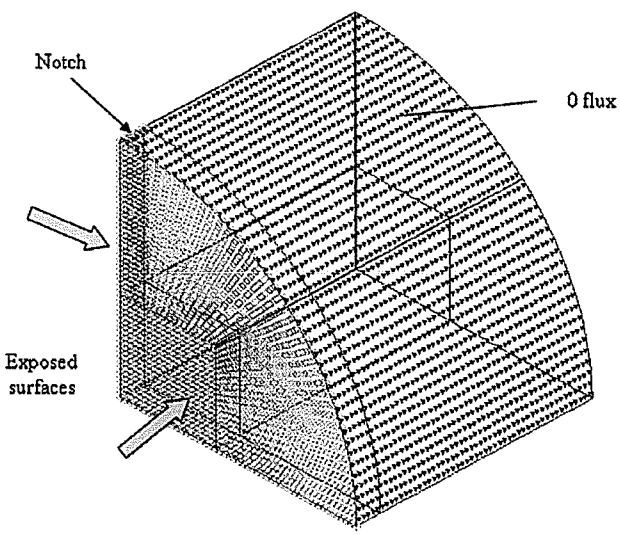

Fig. 4. Geometry and applied boundary conditions for the specimen with notch of 5 mm length and 0.2 mm width.

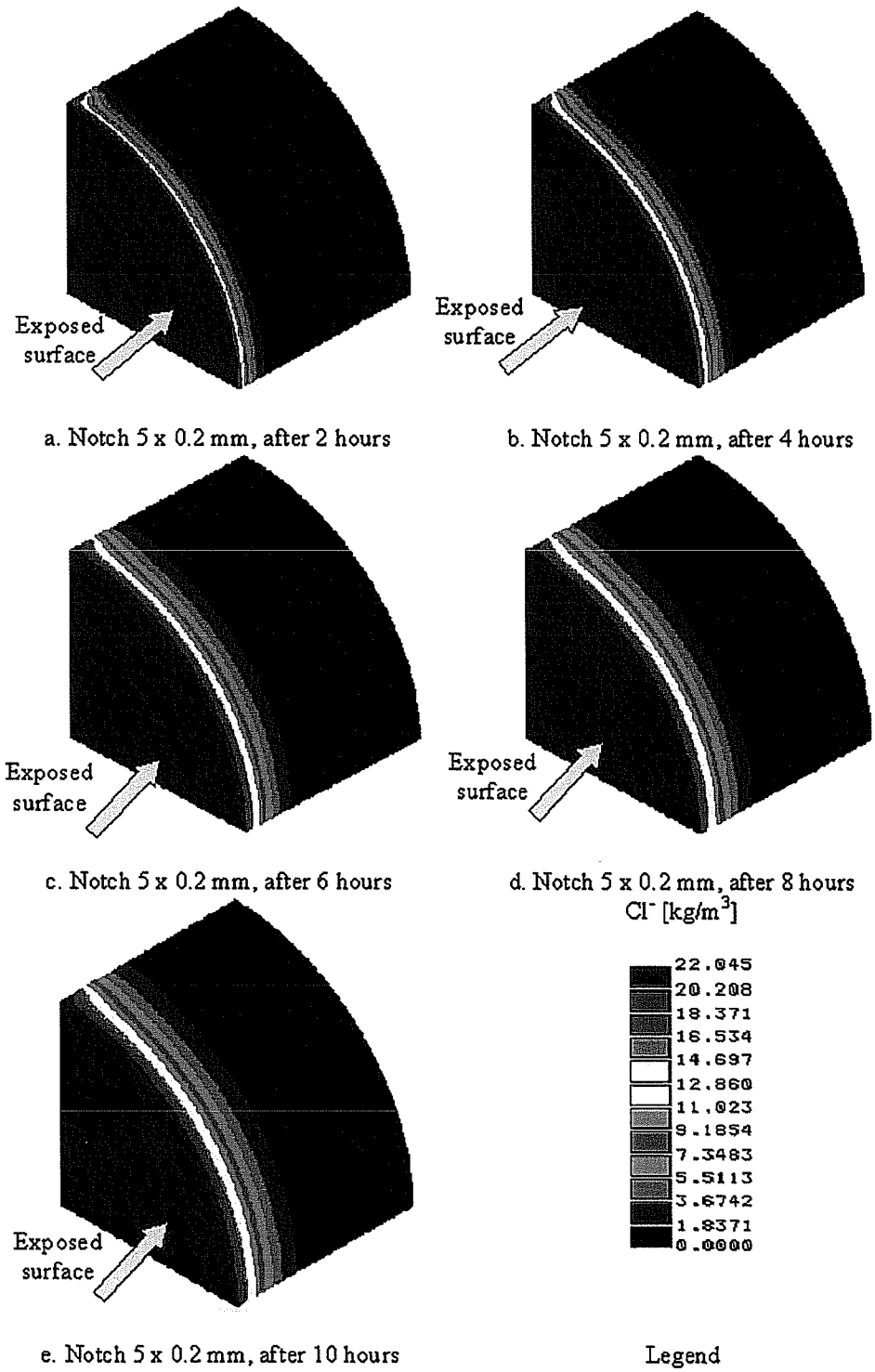

Fig. 5. Evolution of chloride penetration in time for the notched specimen 5 × 0.2 mm.

concentration on the notch edges and on the exposed surface to the chloride solution, Fig. 4.

The values for the diffusion coefficients were determined experimentally from the migration tests on un-notched specimens[5,32] (see Section 3.3). The non-steady-state migration coefficient D_{nssm} was then corrected in order to take into account the age of the concrete (according with Eq. (5)), and the chloride binding [4].

Based on a study on un-notched specimens, variable diffusion coefficients [43] were considered in accordance with Achari et al. [44], as follow:

$$D = D_0 - A\sqrt{C_{tot}} \quad (7)$$

where C_{tot} represents the total chloride concentration ($C_{tot} = 22.045\ kg/m^3$ for the surfaces exposed to the 10% NaCl solution), $A = 1.467$ the slope of the graph represented by Eq. (7), and $D_0 = 15.554 \times 10^{-12}\ m/s^2$, corresponding to Type 2 concrete.

The simulation time was calculated with Eq. (2) in function of the diffusion coefficient and the mean penetration experimentally obtained. For the notched models the mean penetration depth was calculated in the un-notched part of the specimen, and corresponding to 10 h experiment. The steps of the transient analysis were chosen in accordance with the time intervals considered in the experiments (2, 4, 6, 8, and 10 h).

4.3. Results and discussions

Fig. 5 presents the chloride profile for the 5 × 0.2 mm notch model after 2, 4, 6, 8, and 10 h. The chloride penetration was interrogated in a series of position points with 1 mm step up to 10 mm distance from the notch and with a 5 mm step at greater distance from the notch. A polynomial interpolation was applied in order to determine the penetration corresponding to the same concentration that was experimental obtained by using the silver nitrate solution ($1.183\ kg_{Cl^-}/m^3$).

In Fig. 6 the experimentally obtained chloride penetration profiles are plotted, together with the numerical simulation results obtained with the finite element method. A good agreement was obtained between experimental and numerical values in case of notch width of 0.2 mm and notch length of 10 mm (Fig. 6b), 15 mm length (Fig. 6c) and 20 mm (Fig. 6d), and this for almost all time intervals, excepting the 10 h interval. Close to the notch larger deviations can also be noticed in several cases. For the model with a notch of 5 mm length and 0.2 mm width (Fig. 6a) the experimental and numerical chloride penetrations correspond fairly well near to the notch except after 10 h. For this model the numerical results underestimate the chloride penetration in the region far from the notch for 2, 4 and 6 h time interval.

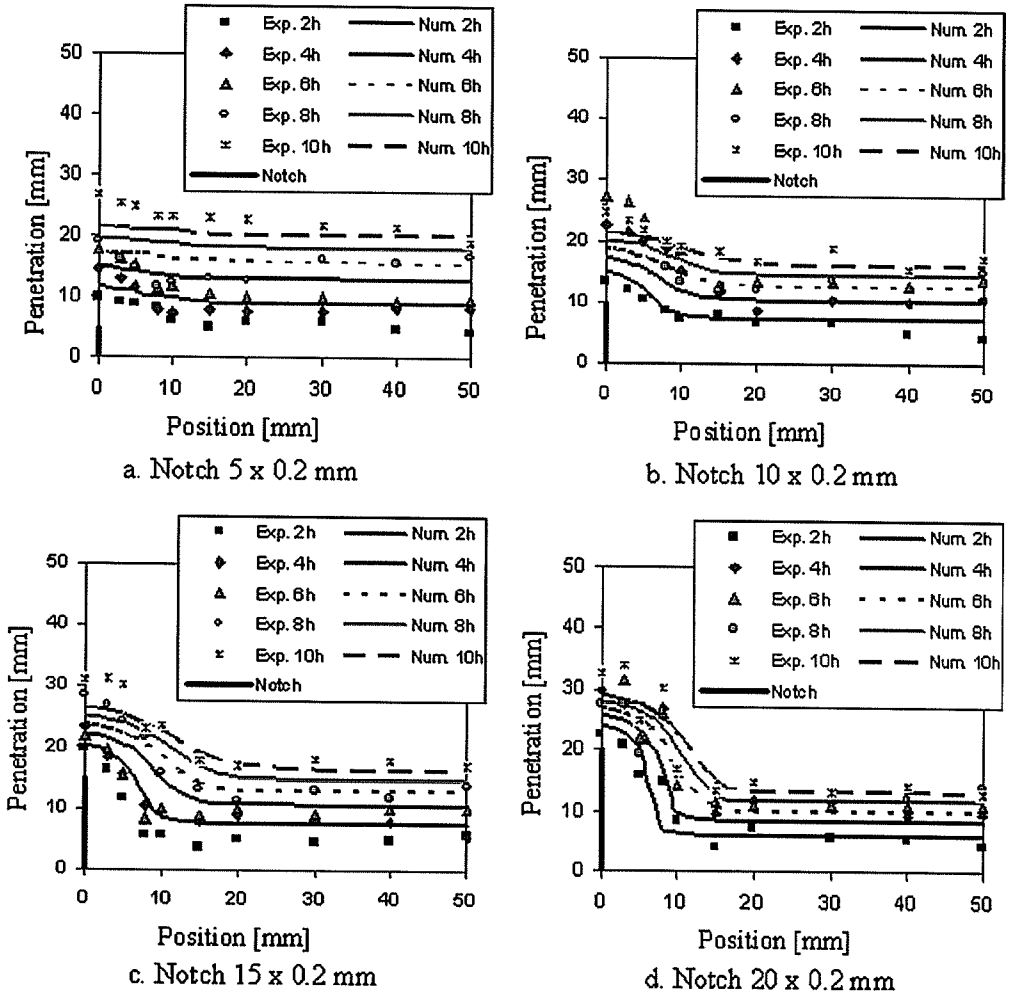

Fig. 6. Comparison between experimental and numerical simulation results on chloride penetration for notched specimen 5 × 0.2 mm.

Both for experiments and simulations the maximum penetration depth is increasing with the increasing of the test duration and with increasing notch depth. The increased penetration depth for an increasing notch depth is more pronounced for longer test durations. This could be attributed to variations related to the test method, such as the accuracy of the measurement of the penetration depth. The influence of the crack width is less pronounced. By studying Tables 3–5, it even seems that a smaller crack width leads to a higher penetration depth.

The higher penetration in experiments near the notches can be possibly explained by the presence of microcracks, e.g. due to hydration and shrinkage of the concrete.

5. Conclusions

In this paper, the influence of artificial cracks, so-called notches, with different crack widths and crack depths on the chloride penetration is experimentally and numerically studied. The chloride penetration was determined by means of the CTH test (NT BUILD 492) using an electrical field. Some final conclusions can be made:

- a higher penetration of chlorides is obtained at the notch tip in comparison with the 'un-cracked' part of the test specimens,
- the penetration depth is increasing with an increasing notch depth. This effect is more pronounced for longer test durations,
- the influence of the notch width is not clear. Further research is needed to clarify the influence of the notch width.

Numerical simulation based on a finite element method represents a good choice for modelling the chloride penetration using a concentration dependent diffusion coefficient and a transient analysis.

It can be concluded that the numerical results agree fairly well with experimental results obtained from migration test for the notched specimens.

Acknowledgements

This work was done in the framework of Bilateral Scientific Agreement between Ghent University, Belgium and "Politehnica" University of Timisoara, Romania, project "Numerical simulation of the influence of crack formation on chloride penetration in reinforced concrete". Also the financial support of the FWO-Flanders is greatly acknowledged.

References

[1] Cady PD, Weyers RE. Chloride penetration and the deterioration of concrete bridge decks. Cement Concr Aggr 1983;5(2):81–7.
[2] Gowripalan N, Sirivivatnanon V, Lim CC. Chloride diffusivity of concrete cracked in flexure. Cement Concr Res 2000;30:725–30.
[3] Win PP, Watanabe M, Machida M. Penetration profile of chloride ion in cracked reinforced concrete. Cement Concr Res 2004;34: 1073–9.
[4] Meijers SJH. Computational modelling of chloride ingress in concrete, PhD Thesis, Delft University Press, 2003.
[5] Tang L, Nilsson L-O. A numerical method for prediction of chloride penetration into concrete structures. In: Jennings H et al., editors. The modelling of microstructure and its potential for studying transport properties and durability. Kluwer Academic Press Publishers; 1996. p. 539–52.
[6] Truc O, Jean-Pierre Olliviera J-P, Nilsson L-O. Numerical simulation of multi-species transport through saturated concrete during a migration test – MsDiff code. Cement Concr Res 2000;30:1581–92.
[7] Martin-Perez B, Pantazopoulou SJ, Thomas MDA. Numerical solution of mass transport equations in concrete structures. Comput Struct 2001;79:1251–64.
[8] Wang Y, Li L-Y, Page CL. Modelling of chloride ingress into concrete from a saline environment. Build Environ 2005;40:1573–82.
[9] De Schutter G. Quantification of the influence of cracks in concrete structures on carbonation and chloride penetration. Mag Concr Res 1999;51(6):427–35.
[10] De Schutter G. Influence of early age thermal cracking on durability of massive concrete structures in marine environment. In: Lacasse MA, Vanier DJ, editors. Durability of building materials and components 8, vol. 1. Ottawa: NRC Research Press; 1999. p. 129–38.
[11] De Schutter G, Audenaert K. Penetration of aggressive substances in cracked concrete. In: Proceedings of the IVth international symposium on concrete for a sustainable agriculture, Gent, 2002. p. 123–9.
[12] Tang L. Chloride transport in concrete – measurement and prediction. Publication P96-6. Göteborg: Chalmers University of Technology; 1996.
[13] Chatterji S. On the non-applicability of unmodified Fick's laws to ion transport through cement based materials. In: Nilsson LO, Ollivier JP, editors. Chloride penetration into concrete. St-Remy-les-Chevreuse; 1995. p. 64–73.
[14] Wang K, Jansen D, Shah S, Karr A. Permeability study of cracked concrete. Cement Concr Res 1997;27(3):381–93.
[15] Aldea C-M, Shah S, Karr A. Permeability of cracked concrete. Mater Struct 1999;32(3):370–6.
[16] Chen J, Lin K, Young S. Effects of crack width and permeability on moisture induced damage of pavements. ASCE J Mater Civil Eng 2004;16(3):276–82.
[17] Song H, Kwon S, Byun K, Park C. Predicting carbonation in early-aged cracked concrete. Cement Concr Res 2006;36(5):979–89.
[18] Brühwiler E, Wittmann F. The wedge splitting test, a new method of performing stable fracture mechanics tests. Eng Fract Mech 1990;35(1–3):117–25.
[19] Leite J, Slowik V, Mihashi H. Computer simulation of fracture processes of concrete using mesolevel models of lattice structures. Cement Concr Res 2004;34(6):1025–33.
[20] Karihaloo B, Abdalla H, Xiao Q. Deterministic size effect in the strength of cracked concrete structures. Cement Concr Res 2006;36(1):171–88.
[21] Pease B, Skocek J, Geiker M, Stang H, Weiss J. The wedge splitting test: influence of aggregate size and water-to-cement ratio. In: Audenaert K, Marsavina L, De Schutter G, editors. International RILEM workshop on transport mechanisms in cracked concrete, Acco Leuven, 2007. p. 111–22.
[22] Reinhardt H. Fluid transport in wedge-split concrete. In: Audenaert K, Marsavina L, De Schutter G, editors, International RILEM workshop on transport mechanisms in cracked concrete, Acco Leuven, 2007. p. 13–8.
[23] Li CQ. Initiation of chloride-induced reinforcement corrosion in concrete structural members – experimentation. ACI Struct J 2001;98(4):502–10.
[24] Mohammed T, Otsuki N, Hisada M, Shibata T. Effect of crack width and bar types on corrosion of steel in concrete. ASCE J Mater Civil Eng 2001;13(3):194–201.

[25] Granju J-L, Balouch S. Corrosion of steel fibre reinforced concrete from the cracks. Cement Concr Res 2005;35(3):572–7.
[26] Kato E, Kato Y, Uomoto T. Development of simulation model of chloride ion transportation in cracked concrete. J Adv Concr Technol 2005;3(1):85–94.
[27] Mu R, Miao C, Luo X, Sun W. Interaction between loading, freeze–thaw cycles, and chloride salt attack of concrete with and without steel fiber reinforcement. Cement Concr Res 2002;32(7):1061–6.
[28] Ismail M, Toumi A, François R, Gagné R. Effect of crack opening on the local diffusion of chloride in inert materials. Cement Concr Res 2004;34(4):711–6.
[29] Schlangen E, Yoon I-S, De Rooij M. Measurement of chloride ingress in cracked concrete. In: Audenaert K, Marsavina L, De Schutter G, editors, Proceedings of the int. RILEM workshop transport mechanisms in cracked concrete, Acco Leuven, 2007. p. 19–25.
[30] Audenaert K, De Schutter G, Marsavina L, Boel V. Influence of cracks and crack width on penetration depth of chlorides in concrete. In: 1st international conference on heritage and constructions in coastal and marine environment, Lisbon, Portugal, 28–30 January 2008, abstract accepted.
[31] Tang L, Nilsson L-O. Rapid determination of chloride diffusivity of concrete by applying an electric field. ACI Mater J 1992;89:49–53.
[32] NT BUILD 492. Concrete, mortar and cement-based repair materials: chloride migration coefficient from non-steady-state migration experiments, 1999.
[33] Audenaert K. Transport mechanisms in self-compacting concrete in relation to carbonation and chloride penetration (in Dutch). PhD Thesis, Ghent University, 2006.
[34] Audenaert K, Boel V, De Schutter G. Chloride penetration in self compacting concrete by cyclic immersion. In: First international symposium on design, performance and use of self consolidating concrete, Changsha, China, May 26–28, 2005.
[35] Otsuki N, Nagataki S, Nakashita K. Evaluation of $AgNO_3$ solution spray method for measurement of chloride penetration into hardened cementations matrix materials. ACI Mater J 1992;89(6):587–92.
[36] Tang L, Sorensen H. Precision of the Nordic test methods for measuring chloride diffusion/migration coefficients of concrete. Mater Struct 2001;34:479–85.
[37] Bamforth P. The derivation of input data for modelling chloride ingress from eight year UK coastal exposure trials. Mag Concr Res 1999;51(2):87–97.
[38] Costa A, Appleton J. Chloride penetration into concrete in marine environment – part I: main parameters affecting chloride penetration. Mater Struct 1999;32:252–9.
[39] Costa A, Appleton J. Chloride penetration into concrete in marine environment – part II: prediction of long term chloride penetration. Mater Struct 1999;32:354–9.
[40] Mangat P, Molloy B. Prediction of long term chloride concentration in concrete. Mater Struct 1994;27:338–46.
[41] Audenaert K, Boel V, De Schutter G. Chloride migration in self-compacting concrete. In: CONSEC '07, France, 2007.
[42] COSMOS/FFE Thermal, Structural Research and Analysis Corp., Los Angeles, USA, 1999.
[43] Marsavina L, De Schutter G, Audenaert K, Marsavina D, Faur N. The influence of cracks on chloride penetration in concrete structures. Part II: numerical simulation. In: Audenaert K, Marsavina L, De Schutter G, editors. Proceedings of the int. RILEM workshop transport mechanisms in cracked concrete, Acco Leuven, 2007. p. 45–54.
[44] Achari G, Chatterji S, Joshi RC. Evidence of the concentration dependent ionic diffusivity through saturated porous media. In: Nilsson LO, Ollivier JP, editors. Chloride penetration into concrete. St-Remy-les-Chevreuse; 1995. p. 74–6.